Contemporary Mathematics
https://ojs.wiserpub.com/index.php/CM/

Research Article

Quiescent Optical Solitons for Radhakrishnan-Kundu-Lakshmanan Equation with Linear Temporal Evolution

Şebnem Gökdeniz Sıvakcı[1], Yakup Yildirim[2,3*], Aydın Seçer[1], Anjan Biswas[4,5,6,7]

[1]Mathematical Engineering, Yildiz Technical University, 34230, Istanbul, Turkey
[2]Department of Computer Engineering, Biruni University, Istanbul, 34010, Turkey
[3]Mathematics Research Center, Near East University, 99138, Nicosia, Cyprus
[4]Department of Mathematics & Physics, Grambling State University, Grambling, LA, 71245-2715, USA
[5]Department of Physics and Electronics, Khazar University, Baku, AZ, 1096, Azerbaijan
[6]Department of Applied Sciences, Cross-Border Faculty of Humanities, Economics and Engineering, Dunarea de Jos University of Galati, 111 Domneasca Street, Galati, 800201, Romania
[7]Department of Mathematics and Applied Mathematics, Sefako Makgatho Health Sciences University, Medunsa, 0204, South Africa
E-mail: yyildirim@biruni.edu.tr

Received: 27 April 2025; **Revised:** 15 June 2025; **Accepted:** 9 July 2025

Abstract: This study explores novel quiescent optical soliton solutions to the Radhakrishnan-Kundu-Lakshmanan (RKL) equation, a significant model in nonlinear optics. Utilizing three distinct analytical methods, which are the modified extended Tanh-function method, the addendum to Kudryashov method, and the Kudryashov's auxiliary equation method, we derive an array of new quiescent optical soliton solutions, including dark, singular, bright, and bright-dark solitons. The novelty of this work lies in the comprehensive application of these advanced techniques to uncover previously unreported quiescent optical soliton profiles, revealing the inherent diversity and richness of the RKL equation's solution space. The physical significance of these solutions is highlighted through detailed two-dimensional visualizations, offering deeper insights into their structural characteristics and potential implications in nonlinear optics. This work not only expands new analytical perspectives for solving the RKL equation but also contributes to a broader understanding of soliton wave phenomena in complex nonlinear systems.

***Keywords*:** soliton wave, Radhakrishnan-Kundu-Lakshmanan equation, nonlinear chromatic dispersion

MSC: 78A60, 81V80

1. Introduction

Nonlinear wave equations are indispensable tools in the study of complex physical systems, as they model the interplay of various forces that shape wave dynamics [1–5]. These equations provide a mathematical framework to understand phenomena such as the propagation of light in optical fibers, the motion of water waves in shallow or deep fluids, and the intricate behaviors of plasma in high-energy astrophysical and laboratory environments [6–10]. Unlike linear equations, which are limited to describing simple waveforms, nonlinear equations account for interactions between waves, leading to phenomena such as wave steepening, dispersion, and energy localization. These nonlinear effects are essential in capturing the richness of wave behavior observed in nature and technology.

DOI: https://doi.org/10.37256/cm.6420257104

One of the most intriguing outcomes of nonlinear wave equations is the formation of solitary waves or solitons. Solitons are self-reinforcing waveforms that maintain their shape and energy while traveling over long distances. This stability arises from a delicate balance between nonlinearity, which tends to steepen the wave, and dispersion, which tends to spread it out. Solitons are of particular importance because of their practical applications in fields such as optical communication, where they enable high-capacity data transmission, and in hydrodynamics, where they describe wave patterns in oceans and channels. Their robustness also makes them valuable in understanding energy transport in nonlinear media and exploring fundamental wave dynamics.

The Radhakrishnan-Kundu-Lakshmanan (RKL) equation is a prominent example of a nonlinear wave equation that captures the evolution of complex waveforms [11–15]. Originally formulated to describe the propagation of waves in optical fibers, the RKL equation has been extended to other systems with similar nonlinear and dispersive characteristics. The equation incorporates a wide array of physical effects, making it a versatile model for studying nonlinear wave dynamics [16–20]. These effects include nonlinear Chromatic Dispersion (CD), which influences the wavelength-dependent speed of wave components, and linear temporal evolution, describing the time-dependent behavior of waves. The equation also accounts for higher-order dispersion effects, such as third-Order Dispersion (3OD) and fourth-Order Dispersion (4OD), which become significant in ultrashort pulse dynamics. Additional phenomena captured by the RKL equation include self-steepening, where the nonlinear interaction causes the leading edge of a wave to steepen, and the self-frequency shift, which results from the nonlinear interaction between the wave's components. Furthermore, the equation models spatio-temporal dispersion effects, which describe the coupling between spatial and temporal variations in waveforms. Together, these features make the RKL equation a powerful and comprehensive tool for investigating the dynamics of optical solitons and other nonlinear waveforms [21–25].

The study of the RKL equation has been an area of significant interest due to its ability to support diverse solitary wave solutions. Bright solitons, characterized by localized peaks of intensity, arise when nonlinearity balances anomalous dispersion. These solitons are critical in applications like optical fiber communications, where their stability ensures minimal signal degradation. Conversely, dark solitons, which manifest as localized intensity dips on a continuous wave background, emerge under conditions of normal dispersion. Dark solitons have been observed in both optics and hydrodynamics, providing insights into wave dynamics in various media. Singular solitons represent another intriguing class of solutions. These solitons, distinguished by singularities in their profiles, exhibit unique mathematical and physical properties. Hybrid solutions, such as bright-dark solitons, where bright and dark components coexist, add to the diversity of wave phenomena described by the RKL equation. These solutions highlight the richness of nonlinear dynamics and offer potential for novel applications in areas like signal processing and energy localization.

Despite significant progress, identifying novel solitary wave solutions to the RKL equation remains an active and challenging area of research. Each new solution not only enriches the theoretical understanding of nonlinear systems but also offers potential for practical applications. However, the complexity of the RKL equation often necessitates advanced solution techniques to uncover previously unreported waveforms. In this work, we tackle this challenge by employing three analytical methods: the Modified Extended Tanh-Function Method (METFM), the addendum to Kudryashov method, and the Kudryashov auxiliary equation method. These methods are chosen for their robustness and efficiency in solving nonlinear differential equations. By applying these techniques to the RKL equation, we derive a comprehensive set of solitary wave solutions, including dark, bright, singular, and bright-dark solitons.

The application of multiple analytical techniques namely, the METFM, the addendum to Kudryashov method, and the Kudryashov's auxiliary equation method has a significant impact on the diversity and completeness of the solution space uncovered in this study. Each method possesses unique structural capabilities and algebraic formulations, allowing for the extraction of distinct soliton profiles such as dark, singular, bright, and bright-dark solitons. By employing a multi-methodological approach, we ensure a broader exploration of the RKL equation's nonlinear characteristics, leading to the identification of solution families that may remain hidden under a single method framework. This comparative strategy not only validates the robustness and consistency of the results but also highlights the complementary strengths of each method in capturing various dynamical behaviors inherent in the RKL model. Consequently, the combined use of these techniques enriches the overall analytical depth and enhances the physical interpretability of the obtained soliton structures within the context of nonlinear optical systems. Among the three analytical techniques employed in this study,

the Kudryashov's auxiliary equation method demonstrates a comparatively superior performance in terms of solution versatility and computational efficiency. This method offers a structured and systematic framework that simplifies the balancing process and allows for the direct construction of exact solutions without imposing restrictive ansatz assumptions. In contrast, the METFM, while effective in generating standard soliton structures, is more sensitive to initial balancing conditions and often requires additional steps to isolate nontrivial solutions. The addendum to Kudryashov method serves as a valuable enhancement but tends to produce a narrower class of solutions. Overall, the auxiliary equation method not only yields a richer variety of soliton profiles including both singular and compound forms but also facilitates easier algebraic manipulation and implementation. Therefore, it stands out as the most efficient and flexible tool among the applied approaches for analyzing the nonlinear dynamics of the RKL equation.

Although reference [21] explores equation (1) using methods such as the G'/G expansion, F-expansion, and Kudryashov methods, our approach yields distinct analytical structures. While there are similarities in the qualitative behavior of the solutions, such as solitary and periodic waveforms, our results differ in parameter constraints, functional forms, and solution families due to the adopted method. The novelty of this study lies in the derivation of quiescent solitary wave solutions that have not been reported previously in the context of the RKL equation. These solutions expand the equation's known solution space, offering new insights into its dynamics and potential applications. To emphasize the physical significance of these solutions, we provide detailed two-dimensional plots that visually represent their structural and dynamical properties. These visualizations not only aid in understanding the nature of the solutions but also highlight their practical implications, such as in optical communication systems, where the stability and robustness of solitons are paramount. This expanded investigation underscores the richness of the RKL equation and its capacity to model complex nonlinear wave phenomena, paving the way for further exploration and application of its solutions in diverse scientific and engineering domains.

1.1 *Governing model*

The perturbed RKL equation, incorporating nonlinear CD and additional higher-order effects, is given as [21]:

$$iq_t + a\left(|q|^n q\right)_{xx} + b|q|^2 q = i\lambda\left(|q|^2 q\right)_x + i\mu\left(|q|^2\right)_x q + i\delta|q|^2 q_x - i\gamma_1 q_{xxx} - \gamma_2 q_{xxxx} - \gamma_3 q_{xxt} - \gamma_4 q_{xxxt}. \tag{1}$$

In this equation, $q = q(x, t)$ represents the wave profile, which is a function of spatial (x) and temporal (t) variables. Each term in the equation captures a specific physical effect influencing the dynamics of nonlinear wave propagation. The term iq_t describes the linear temporal evolution of the wave profile. It represents the fundamental time-dependent behavior of the wave, capturing how the wave's amplitude and phase vary over time. The term $a\left(|q|^n q\right)_{xx}$ represents nonlinear CD. Here, a quantifies the effect of dispersion that depends on the wave's intensity $|q|^n$, where n is a nonlinearity parameter. This term models the wavelength-dependent speed of the wave components, a key factor in systems such as optical fibers. The term $b|q|^2 q$ arises from the Kerr effect. This term describes how the wave's intensity modifies its refractive index, driving nonlinear phase modulation and contributing to the wave's evolution. The term $i\lambda\left(|q|^2 q\right)_x$ represents self-steepening, where λ is the self-steepening coefficient. This nonlinear effect leads to the steepening of the leading edge of the wave, preventing the formation of shock waves and introducing asymmetry in the wave profile. The term $i\mu\left(|q|^2\right)_x q$ accounts for higher-order dispersion effects. The coefficient μ quantifies the contribution of these effects, which are particularly significant in ultrashort pulse dynamics, where the interplay of nonlinearity and dispersion becomes complex. The term $i\delta|q|^2 q_x$ stems from the self-frequency shift phenomenon, where δ quantifies the effect. This term models the redshift of the wave's frequency due to nonlinear interactions, commonly observed in optical solitons. The terms $-i\gamma_1 q_{xxx}$ and $-\gamma_2 q_{xxxx}$ represent 3OD and 4OD, respectively. Here, γ_1 and γ_2 are coefficients quantifying the effects of these higher-order dispersions. These terms are essential for capturing the behavior of waves in systems where higher-order dispersion plays a dominant role, such as in ultrafast optics. The terms $-\gamma_3 q_{xxt}$ and $-\gamma_4 q_{xxxt}$ describe spatio-temporal dispersion effects. These terms, characterized by the coefficients γ_3 and γ_4, model the coupling between spatial

and temporal variations in the wave profile. Such effects are crucial in describing the propagation of waves in media with significant spatio-temporal interactions.

When specific parameters are set to zero ($n = \mu = \delta = \gamma_2 = \gamma_3 = \gamma_4 = 0$), the equation reduces to the standard RKL equation [11–20]. This familiar form captures the essential dynamics of nonlinear wave propagation without the additional higher-order effects, making it a foundational model for studying solitary waves in simpler contexts. This generalized form of the RKL equation provides a versatile framework for analyzing the rich dynamics of nonlinear wave systems, accounting for both fundamental and higher-order effects. Its comprehensive nature allows researchers to explore a wide range of physical phenomena and identify novel wave structures in diverse applications.

The organization of the paper is structured to guide readers through the theoretical derivation, analysis, and discussion of the results systematically: Section 2 is dedicated to exploring the derivation of novel quiescent solitons using three distinct analytical approaches: The METFM is employed to derive exact soliton solutions by transforming the nonlinear differential equation into a more manageable form. The method introduces modifications to the traditional tanh-function approach to improve its versatility and applicability in nonlinear systems. The detailed step-by-step implementation of this method, including its assumptions, mathematical transformations, and the derivation process, is provided to ensure reproducibility. This section presents an augmentation of Kudryashov's classical method to address nonlinear equations that feature complex behaviors, such as quiescent solitons. The refinements enhance the robustness of the approach in deriving closed-form solutions. Each step is meticulously documented, including the selection of trial functions, the derivation of necessary parameter constraints, and the interpretation of the resulting soliton solutions. Here, the auxiliary equation method is introduced as a complementary tool for generating soliton solutions. The paper outlines the construction of auxiliary equations and how they are systematically used to uncover a broad class of solutions. Detailed derivations highlight the theoretical framework and the conditions required for the solitons' existence. This section emphasizes the theoretical underpinnings of these methods, their mathematical rigor, and their effectiveness in addressing the governing nonlinear Schrödinger equation. It also compares the strengths and limitations of each approach, providing a comprehensive understanding of their applicability in soliton theory. Section 3 presents a detailed analysis of the soliton solutions obtained using the methods described in Section 2. The results are visualized through a series of figures (Figures 1-4), each focusing on a specific type of soliton: In Figure 1, the characteristics and dynamics of dark solitons are depicted, showcasing their intensity profiles and the conditions under which they emerge. The discussion includes the influence of key parameters such as the nonlinearity coefficient and temporal evolution on the soliton's stability and propagation. In Figure 2 illustrates singular solitons, highlighting their distinctive peaked profiles and the mathematical conditions ensuring their existence. The paper delves into their physical relevance, particularly in optical systems, and discusses the potential challenges in realizing these solutions experimentally. The bright soliton solutions are depicted in Figure 3, showcasing their localized energy concentration and smooth profiles. The discussion addresses their formation, stability criteria, and the impact of perturbations on their propagation dynamics. Figure 4 introduces a hybrid soliton structure, combining bright and dark soliton characteristics. The analysis explores the conditions leading to such straddled configurations and discusses their potential applications in complex optical communication systems. The discussion section ties the results back to the theoretical methods introduced in Section 2, highlighting the consistency and physical significance of the solutions. It also includes a comparative analysis of the solitons, focusing on their unique features, stability, and potential applications in nonlinear optics. Section 4 synthesizes the key findings of the paper, emphasizing the novelty and significance of the derived soliton solutions. It reiterates the effectiveness of the METFM, the addendum to Kudryashov method, and the Kudryashov's auxiliary equation method in addressing the nonlinear Schrödinger equation. Furthermore, it highlights the broader implications of the results for advancing soliton theory and applications in optical systems. Suggestions for future work are provided, including extending the methods to other forms of nonlinear equations and exploring experimental validations of the theoretical findings.

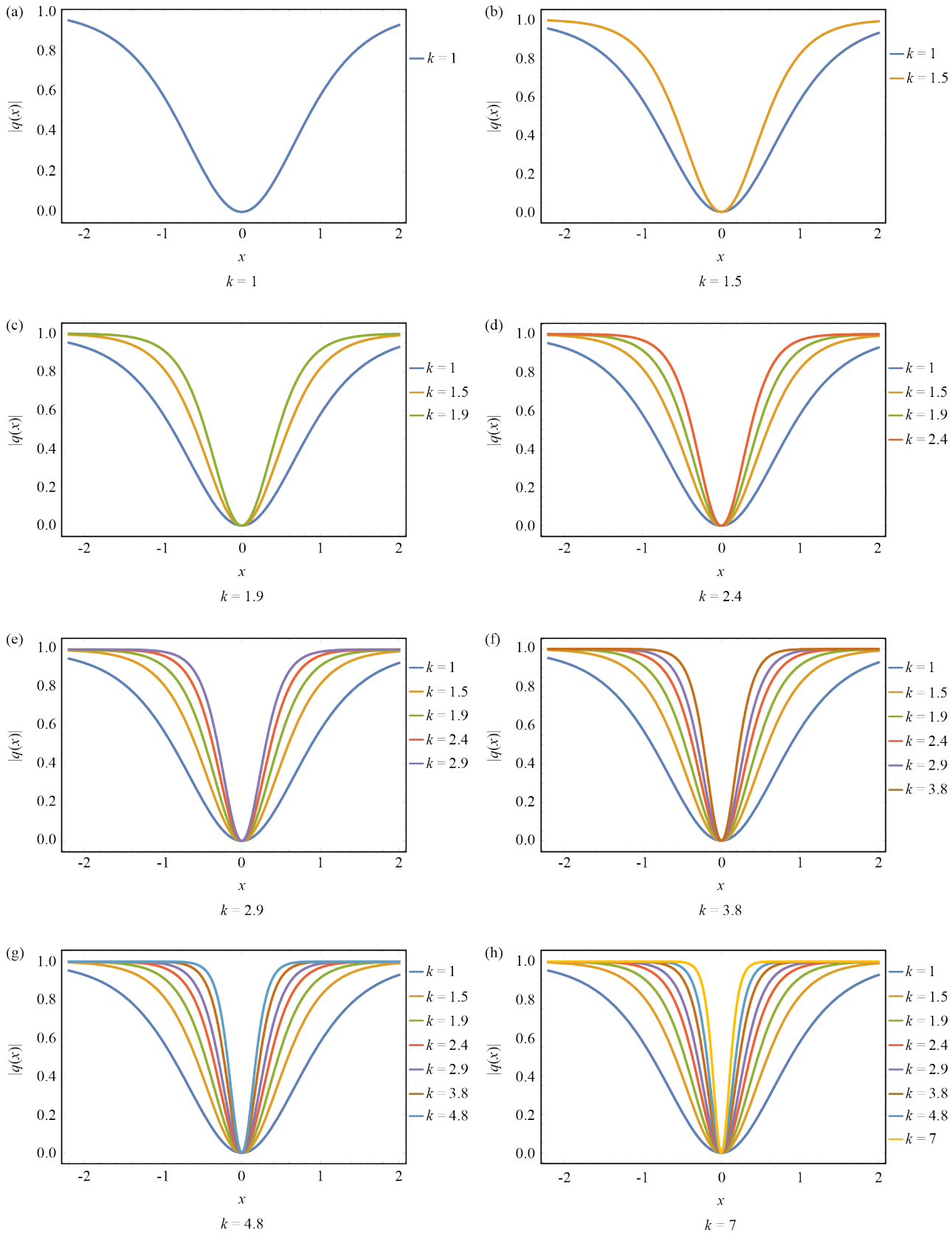

Figure 1. A dark soliton with an emphasis on its amplitude

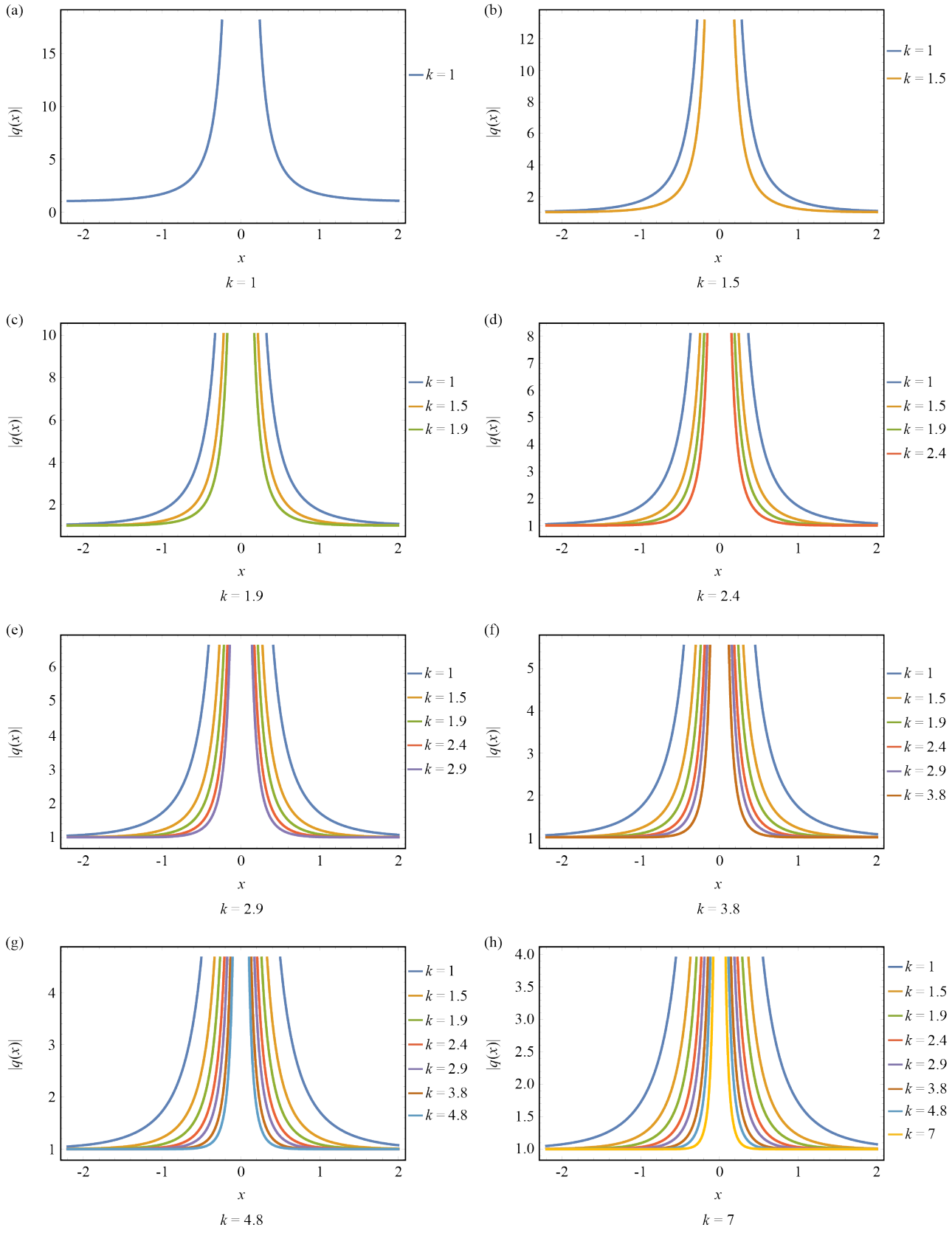

Figure 2. A singular soliton with an emphasis on its amplitude

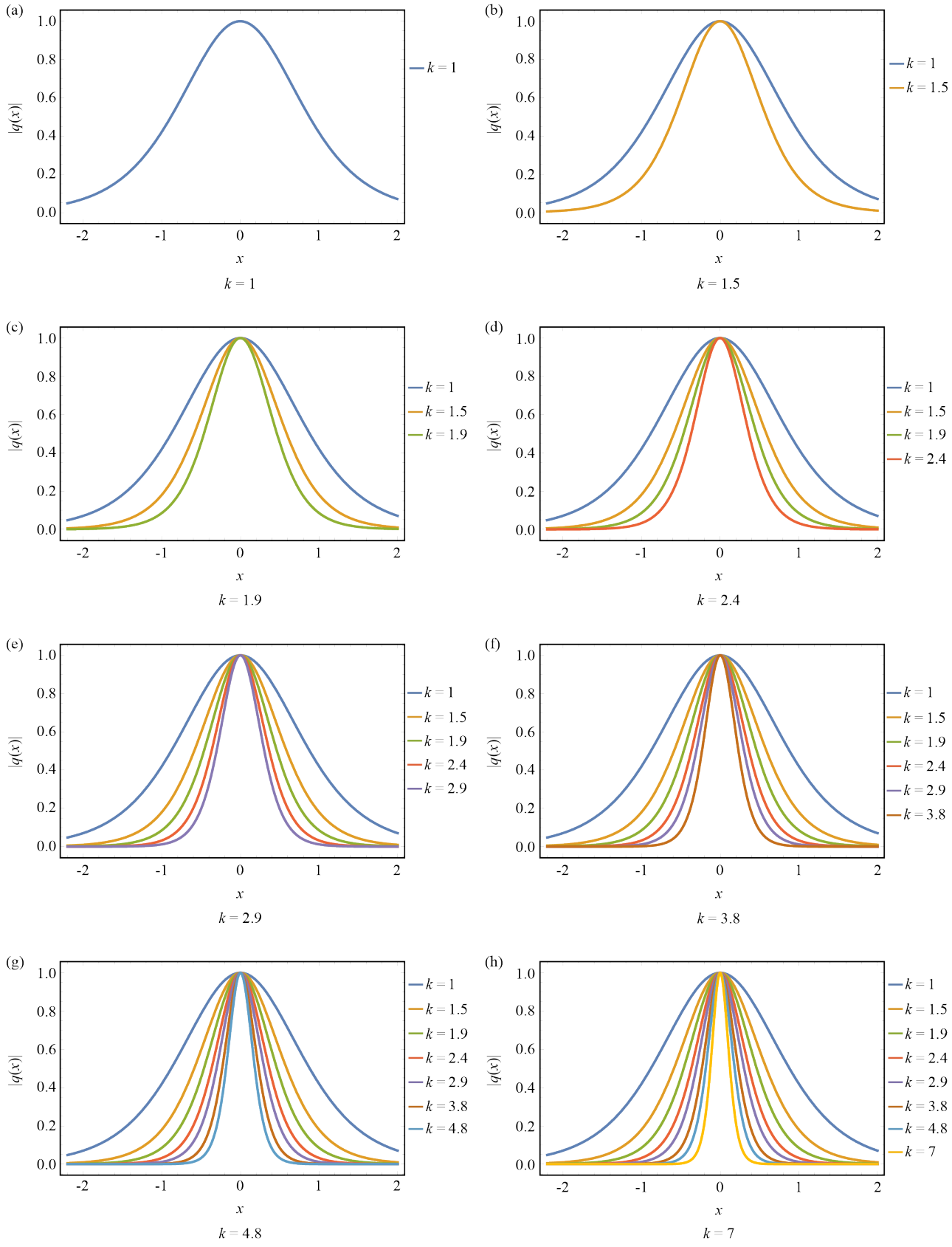

Figure 3. A bright soliton with an emphasis on its amplitude

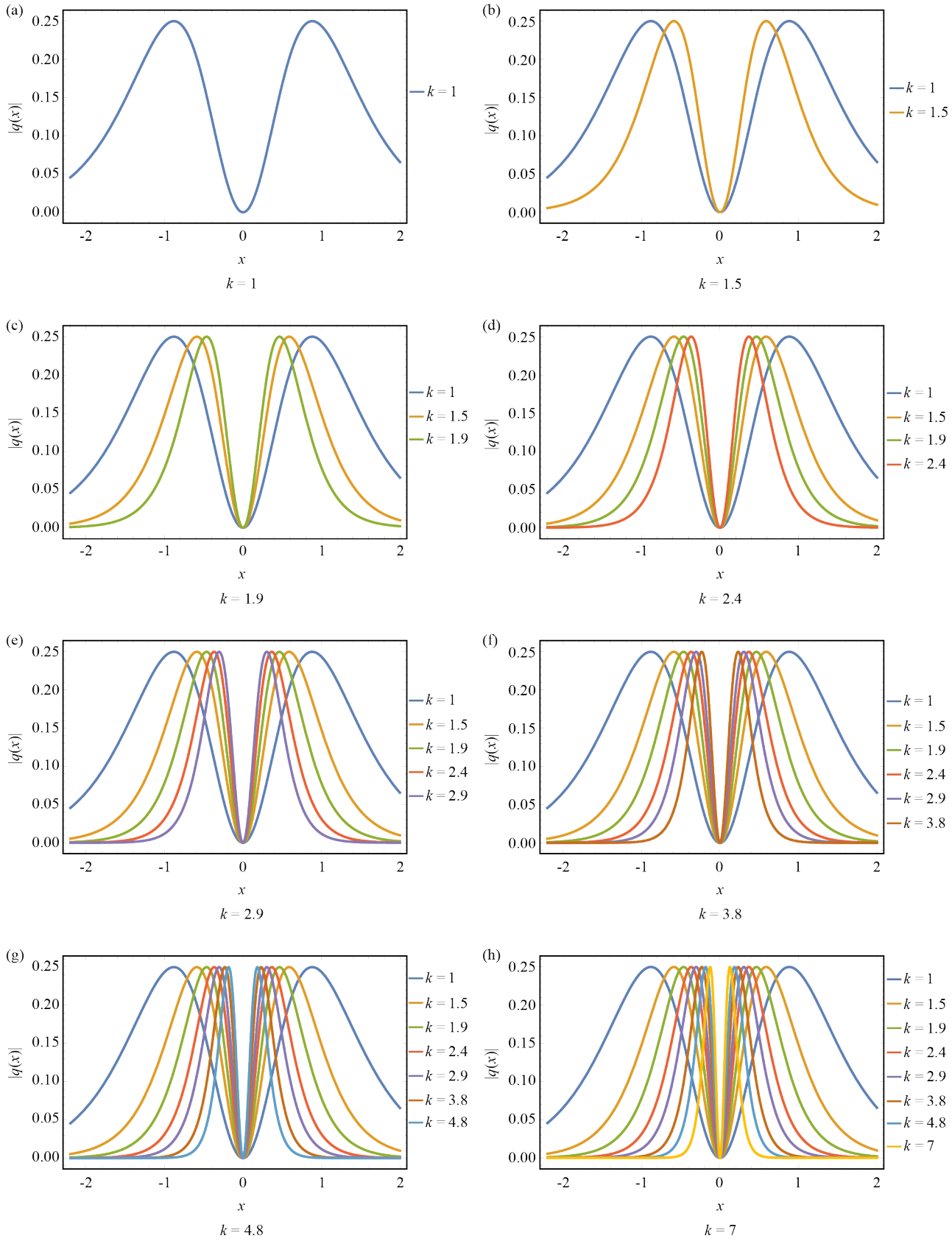

Figure 4. A straddled bright-dark soliton with an emphasis on its amplitude

2. Quiescent solitons

The quiescent soliton profile is fundamental to understanding the behavior of soliton solutions in the context of the RKL equation. This section provides a detailed breakdown of each component and the significance of the derived expressions.

The soliton profile is expressed as:

$$q(x,t) = U(kx)e^{i(\omega t+\theta)}, \tag{2}$$

where $q(x,t)$ represents the soliton solution, a complex-valued function describing the amplitude and phase of the wave. $U(kx)$ is a real-valued function representing the spatial profile of the soliton. The argument kx indicates that the profile is scaled by the inverse width parameter k, directly affecting the soliton's width and localization. $e^{i(\omega t+\theta)}$ introduces a phase factor with angular frequency ω and phase constant θ. This phase component governs the soliton's oscillatory nature in time. The term $U(kx)$ implies that the soliton width scales inversely with k. Larger k values lead to narrower soliton profiles, while smaller k values produce broader solitons. This parameter plays a critical role in modulating soliton characteristics such as peak amplitude and energy distribution. The frequency ω is directly related to the soliton's wavenumber, controlling the temporal oscillations of the soliton. A larger ω results in faster oscillations, impacting the soliton's stability and interaction with the background medium. The phase shift θ provides an additional degree of freedom, influencing the initial soliton phase. This parameter is essential when considering soliton interactions and phase-sensitive applications like optical modulators.

To determine the explicit form of the soliton profile, Eq. (2) is substituted into the RKL equation (1). This substitution separates the real and imaginary parts of the equation, leading to two critical conditions:

$$\gamma_2 k^4 UU^{(iv)} - \gamma_3 k^2 \omega UU'' + ak^2 n(n+1)U^n (U')^2 + ak^2 (n+1)U^{1+n}U'' - \omega U^2 + bU^4 = 0, \tag{3}$$

and

$$k^3(\gamma_1 + \gamma_4\omega)UU''' - k(3\lambda + 2\mu + \delta)U^3U' = 0. \tag{4}$$

To achieve integrability, it is necessary to have:

$$n = 1, \tag{5}$$

$$\gamma_1 + \gamma_4\omega = 0, \tag{6}$$

and

$$3\lambda + 2\mu + \delta = 0. \tag{7}$$

The application of these modifications to the system results in a revised version of the governing equation (1), which reads:

$$iq_t + a\left(|q|\,q\right)_{xx} + b\,|q|^2 q = i\lambda\left(|q|^2 q\right)_x + i\mu\left(|q|^2\right)_x q + i\delta\,|q|^2 q_x - i\gamma_1 q_{xxx} - \gamma_2 q_{xxxx} - \gamma_3 q_{xxt} - \gamma_4 q_{xxxt}. \tag{8}$$

Following this, Eq. (3) reduces to:

$$\gamma_2 k^4 U^{(iv)} - \gamma_3 \omega k^2 U'' + 2ak^2 (U')^2 + 2ak^2 UU'' - \omega U + bU^3 = 0. \tag{9}$$

2.1 *Modified extended Tanh-function method*

The METFM distinguishes itself from classical methods by offering enhanced flexibility and broader applicability to nonlinear Partial Differential Equations (PDEs). Key innovations include: Unlike the standard Tanh-function method, the METFM incorporates a more adaptable trial solution, allowing for the construction of soliton profiles that capture higher-order nonlinear effects and complex dispersive characteristics. This expanded ansatz accommodates mixed soliton structures (e.g., bright-dark solitons) and singular solutions, which are challenging to derive using traditional approaches. The METFM effectively addresses equations with cubic-quartic or higher-order nonlinearities, a domain where classical methods often fall short. This makes it invaluable for models like the RKL equation, where multiple nonlinear and dispersive terms interact simultaneously. By modifying the transformation functions, the METFM can derive bright, dark, singular, and bright-dark solitons within a unified framework. This versatility is crucial for systems where diverse soliton behaviors emerge under different parameter regimes.

The METFM's ability to yield exact soliton solutions carries significant implications for understanding and predicting physical phenomena in nonlinear systems, particularly in optics and photonics. In nonlinear optical fibers and waveguides, solitons play a pivotal role in maintaining stable pulse transmission over long distances. The solutions derived using the METFM describe how solitons evolve under higher-order dispersion and nonlinearity, essential for designing high-speed optical communication systems. The method provides insights into phase-stable solutions, crucial for applications in nonlinear optics, Bose-Einstein condensates, and plasma physics. The exact solutions help in predicting the formation of quiescent (stationary) solitons and their interactions, enhancing the development of advanced photonic devices.

In summary, the METFM's novelty lies in its ability to handle complex nonlinear PDEs with diverse soliton structures, while its physical significance is rooted in its broad applicability to real-world nonlinear phenomena, from optical fiber communications to high-energy plasma dynamics.

We will focus on the model equation [22]:

$$G(q, q_x, q_t, q_{xt}, q_{xx}, ...) = 0, \tag{10}$$

where the spatial-temporal variables x and t are used to describe the optoelectronic wave field $q = q(x, t)$.

Take into account the wave form:

$$q(x, t) = U(\xi), \;\; \xi = \mu(x - vt), \tag{11}$$

where the wave velocity is represented by v, the wave variable by ξ, and the wave width by μ. Hence, equation (10) results in

$$P(U, -\mu v U', \mu U', \mu^2 U'', ...) = 0. \tag{12}$$

Step 1 In the presence of (11), the simplified model confirms the solution structure

$$U(\xi) = A_0 + \sum_{i=1}^{N} \left[A_i R^i(\xi) + \frac{B_i}{R^i(\xi)} \right], \tag{13}$$

through the application of the ancillary equation

$$R'(\xi) = \Omega + R^2(\xi). \tag{14}$$

Thus, we arrive at the soliton wave profiles.
Dark soliton solution:

$$R_1(\xi) = -\sqrt{-\Omega}\tanh(\sqrt{-\Omega}\xi), \tag{15}$$

Singular soliton solution:

$$R_2(\xi) = -\sqrt{-\Omega}\coth(\sqrt{-\Omega}\xi), \tag{16}$$

Complexion solution:

$$R_3(\xi) = -\sqrt{-\Omega}\left(\tanh(2\sqrt{-\Omega}\xi) + i\,\mathrm{sech}(2\sqrt{-\Omega}\xi)\right), \tag{17}$$

Dark soliton solution:

$$R_4(\xi) = \frac{\Omega - \sqrt{-\Omega}\tanh(\sqrt{-\Omega}\xi)}{1 + \sqrt{-\Omega}\tanh(\sqrt{-\Omega}\xi)}, \tag{18}$$

Straddled soliton solution:

$$R_5(\xi) = \frac{\sqrt{-\Omega}(5 - 4\cosh(2\sqrt{-\Omega}\xi))}{3 + 4\sinh(2\sqrt{-\Omega}\xi)}, \tag{19}$$

Singular periodic solutions:

$$R_6(\xi) = \sqrt{\Omega}\tan(\sqrt{\Omega}\xi), \tag{20}$$

$$R_7(\xi) = -\sqrt{\Omega}\cot(\sqrt{\Omega}\xi), \tag{21}$$

$$R_8(\xi) = \sqrt{\Omega}\left(\tan\left(2\sqrt{\Omega}\xi\right) + \sec\left(2\sqrt{\Omega}\xi\right)\right), \tag{22}$$

$$R_9(\xi) = -\frac{\sqrt{\Omega}\left(1-\tan(\sqrt{\Omega}\xi)\right)}{1+\tan(\sqrt{\Omega}\xi)}, \tag{23}$$

$$R_{10}(\xi) = \frac{\sqrt{\Omega}\left(4-5\cos(2\sqrt{\Omega}\xi)\right)}{3+5\sin(2\sqrt{\Omega}\xi)}. \tag{24}$$

Step 2 Combining (13) and (14) within (12), we establish a system of equations that leads to the determination of the unknown constants in (15) through (24).

Balancing the terms $(U')^2$ or UU'' with U^3 in (9) yields $N = 2$. In this integration process, the solution structure (13) is presented in a simplified form as

$$U(\xi) = A_0 + A_1 R(\xi) + \frac{B_1}{R(\xi)} + A_2 R(\xi)^2 + \frac{B_2}{R(\xi)^2}. \tag{25}$$

The combination of (25) with (14) into (9) leaves us with the equations:

$$120B_2\Omega^4k^4\gamma_2 + 20B_2^2\Omega^2ak^2 + B_2^3b = 0, \tag{26}$$

$$24B_1\Omega^4k^4\gamma_2 + 24B_1B_2\Omega^2ak^2 + 3B_1B_2^2b = 0, \tag{27}$$

$$240B_2\Omega^3k^4\gamma_2 + 12A_0B_2\Omega^2ak^2 + 6B_1^2\Omega^2ak^2 - 6B_2\Omega^2k^2\omega\gamma_3 + 32B_2^2\Omega ak^2 + 3A_0B_2^2b + 3B_1^2B_2b = 0, \tag{28}$$

$$40B_1\Omega^3k^4\gamma_2 + 4A_0B_1\Omega^2ak^2 + 4A_1B_2\Omega^2ak^2 - 2B_1\Omega^2k^2\omega\gamma_3 + 36B_1B_2\Omega ak^2 + 6A_0B_1B_2b + 3A_1B_2^2b + B_1^3b = 0, \tag{29}$$

$$136B_2\Omega^2k^4\gamma_2 + 16A_0B_2\Omega ak^2 + 8B_1^2\Omega ak^2 - 8B_2\Omega k^2\omega\gamma_3 + 12B_2^2ak^2 + 3A_0^2B_2b + 3A_0B_1^2b$$
$$+ 6A_1B_1B_2b + 3A_2B_2^2b - B_2\omega = 0, \tag{30}$$

$$16B_1\Omega^2k^4\gamma_2 + 4A_0B_1\Omega ak^2 + 4A_1B_2\Omega ak^2 - 2B_1\Omega k^2\omega\gamma_3 + 12B_1B_2ak^2 + 3A_0^2B_1b + 6A_0A_1B_2b$$
$$+ 3A_1B_1^2b + 6A_2B_1B_2b - B_1\omega = 0, \tag{31}$$

$$16A_2\Omega^3k^4\gamma_2 + 4A_0A_2\Omega^2ak^2 + 2A_1^2\Omega^2ak^2 - 2A_2\Omega^2k^2\omega\gamma_3 + 16B_2\Omega k^4\gamma_2 + 4A_0B_2ak^2 + 2B_1^2ak^2$$
$$- 2B_2k^2\omega\gamma_3 + A_0^3b + 6A_0A_1B_1b + 6A_0A_2B_2b + 3A_1^2B_2b + 3A_2B_1^2b - A_0\omega = 0, \tag{32}$$

$$16A_1\Omega^2k^4\gamma_2 + 12A_1A_2\Omega^2ak^2 + 4A_0A_1\Omega ak^2 - 2A_1\Omega k^2\omega\gamma_3 + 4A_2B_1\Omega ak^2 + 3A_0^2A_1b + 6A_0A_2B_1b$$

$$+ 3A_1^2B_1b + 6A_1A_2B_2b - A_1\omega = 0, \tag{33}$$

$$136A_2\Omega^2k^4\gamma_2 + 12A_2^2\Omega^2ak^2 + 16A_0A_2\Omega ak^2 + 8A_1^2\Omega ak^2 - 8A_2\Omega k^2\omega\gamma_3 + 3A_0^2A_2b + 3A_0A_1^2b$$

$$+ 6A_1A_2B_1b + 3A_2^2B_2b - A_2\omega = 0, \tag{34}$$

$$40A_1\Omega k^4\gamma_2 + 36A_1A_2\Omega ak^2 + 4A_0A_1ak^2 - 2A_1k^2\omega\gamma_3 + 4A_2B_1ak^2 + 6A_0A_1A_2b + A_1^3b + 3A_2^2B_1b = 0, \tag{35}$$

$$240A_2\Omega k^4\gamma_2 + 32A_2^2\Omega ak^2 + 12A_0A_2ak^2 + 6A_1^2ak^2 - 6A_2k^2\omega\gamma_3 + 3A_0A_2^2b + 3A_1^2A_2b = 0, \tag{36}$$

$$24A_1k^4\gamma_2 + 24A_1A_2ak^2 + 3A_1A_2^2b = 0, \tag{37}$$

$$120A_2k^4\gamma_2 + 20A_2^2ak^2 + A_2^3b = 0. \tag{38}$$

Upon solving these equations, one uncovers the outcomes:

$$A_0 = A_2\Omega, \quad A_1 = 0, \quad A_2 = A_2, \quad B_1 = 0, \quad B_2 = 0, \quad k = k,$$

$$a = \frac{3\omega\left(16\Omega k^2\gamma_3 - 5\right)}{32A_2\Omega^2k^2}, \quad b = \frac{15\omega}{8A_2^2\Omega^2}, \quad \gamma_2 = -\frac{\omega\left(4\Omega k^2\gamma_3 - 1\right)}{16\Omega^2k^4}. \tag{39}$$

The inclusion of (39) with the help of (15) into (25) results in the dark soliton solution as:

$$q_1(x,t) = \left(A_2\Omega - A_2\Omega\tanh\left(\sqrt{-\Omega}kx\right)^2\right)e^{i(\omega t+\theta)}. \tag{40}$$

Incorporating both (39) and (16) into (25) leads to the singular soliton solution:

$$q_2(x,t) = \left(A_2\Omega - A_2\Omega\coth\left(\sqrt{-\Omega}kx\right)^2\right)e^{i(\omega t+\theta)}. \tag{41}$$

When (39) is employed with the application of (17) within (25), the complexion solution is obtained as

$$q_3(x,t) = \left(A_2\Omega - A_2\Omega\left(\tanh\left(2\sqrt{-\Omega}kx\right) + \operatorname{sech}\left(2\sqrt{-\Omega}kx\right)i\right)^2\right)e^{i(\omega t+\theta)}. \tag{42}$$

Incorporating both (39) and (18) into (25) leads to the structuring of the dark soliton solution

$$q_4(x,t)\left(A_2\Omega+\frac{A_2\left(\Omega-\sqrt{-\Omega}\tanh\left(\sqrt{-\Omega}kx\right)\right)^2}{\left(1+\sqrt{-\Omega}\tanh\left(\sqrt{-\Omega}kx\right)\right)^2}\right)e^{i(\omega t+\theta)}. \tag{43}$$

When (39) is incorporated with the help of (19) within (25), we retrieve the straddled soliton solution as

$$q_5(x,t)=\left(A_2\Omega-\frac{A_2\Omega\left(5-4\cosh\left(2\sqrt{-\Omega}kx\right)\right)^2}{\left(3+4\sinh\left(2\sqrt{-\Omega}kx\right)\right)^2}\right)e^{i(\omega t+\theta)}. \tag{44}$$

The wave profiles, as characterized in (40) through (44), are defined as

$$\Omega<0. \tag{45}$$

2.2 *Addendum to Kudryashov method*

The addendum to Kudryashov method builds upon the classical Kudryashov approach by refining the handling of nonlinear differential equations, particularly those involving higher-order and mixed nonlinearities. The key novelties include: The addendum introduces an expanded polynomial form for trial solutions, enabling the method to address higher-order nonlinear Schrödinger equations and complex systems with cubic-quartic nonlinearities. This modification allows for more accurate modeling of nonlinear wave phenomena that standard Kudryashov methods might oversimplify. By incorporating additional free parameters into the solution framework, the method achieves greater flexibility in capturing a broader range of soliton behaviors. This enhancement is crucial for modulating soliton amplitude, width, and phase characteristics. Unlike the classical Kudryashov approach, which primarily balances lower-order terms, the addendum extends the balance principle to higher-order derivative and nonlinear interaction terms, enabling the derivation of multi-peak, singular, and composite soliton solutions. The method's refinement allows it to be applied to nonlinear optical systems, plasma physics, and fluid dynamics models, demonstrating its utility across a diverse range of physical problems.

The addendum to Kudryashov method plays a pivotal role in advancing the understanding of nonlinear phenomena, particularly in systems governed by the cubic-quartic Nonlinear Schrödinger (NLS) equation and related models. The method is essential for exploring quiescent optical solitons, such as those found in magneto-optic waveguides and fiber lasers. The derived solutions provide insights into the behavior of bright, dark, and singular solitons, which are fundamental to pulse shaping and stable light transmission in nonlinear optical media. By addressing complex soliton structures, the method aids in predicting soliton interactions, energy transfer, and stability criteria in nonlinear systems. This is particularly relevant for high-power laser systems, nonlinear metamaterials, and Bose-Einstein condensates.

In conclusion, the addendum to Kudryashov method enhances the classical approach by enabling the derivation of complex soliton solutions across various nonlinear models. Its physical significance lies in its broad applicability to modern nonlinear optics, plasma physics, and wave dynamics, offering deeper insights into soliton behavior and energy localization in diverse physical systems.

Step 1 According to the addendum to Kudryashov method, the solution form is constructed as follows [23, 24]:

$$U(\xi)=A_0+\sum_{i=1}^{N}\left[A_iR^i(\xi)\right], \tag{46}$$

where A_i are the parameters to be determined later with $A_N \neq 0$ and $R(\xi)$ is the solution of the following equation:

$$R'(\xi) = \sqrt{R(\xi)^2 (1 - \chi R^{2p}(\xi)) \ln^2(K)}, \qquad 0 < K \neq 1, \tag{47}$$

where χ is an arbitrary constant and p is a positive integer. Moreover, the fucntion $R(\xi)$ has the solution:

$$R(\xi) = \left[\frac{4L}{(4L^2 + \chi)\cosh(\xi p \ln(K)) + (4L^2 - \chi)\sinh(\xi p \ln(K))} \right]^{\frac{1}{p}}, \tag{48}$$

where L is a nonzero constant. Particularly, if $\chi = 4L^2$, the bright soliton is:

$$R(\xi) = \left[\frac{1}{2L} \text{sech}(\xi p \ln(K)) \right]^{\frac{1}{p}}. \tag{49}$$

Step 2 According to the homogeneous balance rule, the relation between p and N is formed as:

Setting $D[\phi(\xi)] = N$, $D[\phi'(\xi)] = N + p$, $D[\phi''(\xi)] = N + 2p$, therefore $D\left[\phi^{(r)}(\xi)\right] = N + rp$, and $D\left[\phi^s(\xi)\phi^{(r)}(\xi)\right] = (s+1)N + rp$.

Step 3 When we substitute (46) and (47) into (9), equating the all coefficients of $R(\xi)$ to zero, then we obtain an algebraic system. Using the homogeneous balance rule, the relation between $U^{(iv)}$ and UU'' from (9) results the equation $N + 4p = 2N + 2p$, thus $N = 2p$ is acquired.

If we put $p = 1$, then $N = 2$. In this case, we have the simplified form as:

$$U(\xi) = A_0 + A_1 R(\xi) + A_2 R(\xi)^2, \tag{50}$$

through the application of the ancillary equation

$$R'(\xi) = \sqrt{R(\xi)^2 (1 - \mu R^2(\xi)) \ln^2(K)}. \tag{51}$$

Thus, we arrive at the soliton wave profiles

$$R(\xi) = \frac{4L}{(4L^2 + \chi)\cosh(\xi \ln(K)) + (4L^2 - \chi)\sinh(\xi \ln(K))}. \tag{52}$$

If $\chi = 4L^2$, the bright soliton is:

$$R(\xi) = \frac{1}{2L} \text{sech}(\xi \ln(K)). \tag{53}$$

The combination of (50) with (51) into (9) leaves us with the equations:

$$A_0\left(A_0^2 b - w\right) = 0, \tag{54}$$

$$\left(\gamma_2 \ln(K)^4 k^4 - k^2\left(-2A_0 a + w\gamma_3\right)\ln(K)^2 + 3bA_0^2 - w\right)A_1 = 0, \tag{55}$$

$$16A_2\gamma_2 \ln(K)^4 k^4 - 4k^2\left(-aA_1^2 + A_2\left(-2A_0 a + w\gamma_3\right)\right)\ln(K)^2 + 3bA_0A_1^2 + 3\left(bA_0^2 - \frac{w}{3}\right)A_2 = 0, \tag{56}$$

$$18A_1\left(-\frac{10\gamma_2 \ln(K)^4 k^4 \chi}{9} + \left(A_2 a + \frac{\chi\left(-2A_0 a + w\gamma_3\right)}{9}\right)k^2 \ln(K)^2 + \frac{\left(A_2A_0 + \frac{A_1^2}{6}\right)b}{3}\right) = 0, \tag{57}$$

$$-120A_2\gamma_2 \ln(K)^4 k^4 \chi + 16\left(-\frac{3a\chi A_1^2}{8} + \left(A_2 a + \frac{3\chi\left(-2A_0 a + w\gamma_3\right)}{8}\right)A_2\right)k^2 \ln(K)^2 + 3A_2 b\left(A_0A_2 + A_1^2\right) = 0, \tag{58}$$

$$3A_1\left(8\gamma_2 k^4 \chi^2 \ln(K)^4 - 8A_2 ak^2 \chi \ln(K)^2 + A_2^2 b\right) = 0, \tag{59}$$

$$A_2\left(120\gamma_2 k^4 \chi^2 \ln(K)^4 - 20A_2 ak^2 \chi \ln(K)^2 + A_2^2 b\right) = 0. \tag{60}$$

Upon solving these equations, one uncovers the outcomes:

$$A_0 = 0, \quad A_1 = 0, \quad A_2 = \frac{20\ln(K)^2 k^2 a\chi}{(16k^2 \ln(K)^2\gamma_3 + 5)b},$$

$$\omega = \frac{640a^2 k^4 \ln(K)^4}{3b\left(16k^2 \ln(K)^2\gamma_3 + 5\right)^2}, \quad \gamma_2 = -\frac{40a^2\left(4k^2 \ln(K)^2\gamma_3 + 1\right)}{3b\left(16k^2 \ln(K)^2\gamma_3 + 5\right)^2}. \tag{61}$$

The inclusion of (61) with the help of (52) into (50) results in the bright soliton solution:

$$q(x,t) = \frac{5\ln(K)^2 k^2 a\chi \operatorname{sech}^2(kx\ln(K))}{(16k^2 \ln(K)^2\gamma_3 + 5)bL^2} e^{\left(\frac{5i}{3}\left(\frac{128\left(\frac{6b\theta\gamma_3^2}{5} + a^2 t\right)k^4 \ln(K)^4 + 96\ln(K)^2 bk^2\theta\gamma_3 + 15b\theta}{b\left(16k^2 \ln(K)^2\gamma_3 + 5\right)^2}\right)\right)}. \tag{62}$$

2.3 *Kudryashov's auxiliary equation method*

The Kudryashov's auxiliary equation method introduces an analytical framework that systematically derives exact soliton solutions by reducing complex nonlinear PDEs to simpler auxiliary equations. This method's novelty lies in several key aspects: Unlike conventional methods that directly tackle nonlinear PDEs, this approach transforms the original equation into an auxiliary Ordinary Differential Equation (ODE). The auxiliary equation has well-known solutions, enabling a more straightforward and structured pathway to soliton solutions. The method employs a general polynomial ansatz for the soliton profile, accommodating a wide variety of nonlinearities (e.g., cubic, quartic, and higher-order). This

flexibility allows for the derivation of bright, dark, singular, and periodic solitons without requiring separate solution strategies for each case. The Kudryashov's method systematically balances nonlinear and dispersive terms by leveraging the auxiliary equation form, simplifying the derivation of soliton solutions. This direct approach eliminates iterative guesswork, making it computationally efficient and precise. The method is not confined to a specific class of PDEs. It can be applied to Nonlinear Schrödinger (NLS) equations, Korteweg-de Vries (KdV) equations, and Boussinesq equations, demonstrating its versatility across diverse nonlinear models.

The method plays a crucial role in advancing the theoretical understanding and practical modeling of nonlinear wave phenomena across multiple fields, particularly in nonlinear optics, fluid dynamics, and plasma physics. In nonlinear optical systems, soliton solutions derived using this method describe stable light pulses that propagate through fibers and waveguides without distortion. This has direct applications in optical communication technologies, where solitons maintain signal integrity over long distances. The auxiliary equation method facilitates the derivation of phase-coherent soliton structures, crucial for modeling quiescent solitons in magneto-optic media and laser cavities. This enables the design of mode-locked lasers and optical switches that rely on soliton dynamics. The method's ability to produce singular solitons highlights its significance in describing energy localization, rogue waves, and shock structures. These phenomena are particularly relevant in plasma physics and fluid dynamics, where energy focusing can lead to critical system instabilities. In fluid dynamics, Kudryashov's method describes soliton interactions and energy transfer in shallow water waves and atmospheric dynamics, offering insights into nonlinear wave breaking, soliton fission, and dispersion management.

The novelty of Kudryashov's auxiliary equation method lies in its ability to transform complex nonlinear PDEs into tractable auxiliary equations, providing a unified framework for deriving diverse soliton solutions. Its physical significance spans nonlinear optics, plasma physics, and fluid dynamics, offering essential tools for modeling and predicting soliton behavior in real-world nonlinear systems.

In the presence of (46), the simplified model confirms the solution structure [25]:

$$U(\xi) = A_0 + A_1 R(\xi) + A_2 R(\xi)^2, \tag{63}$$

through the application of the ancillary equation

$$R'(\xi) = \sqrt{\delta^2 R(\xi)^2 (\chi_1 - \chi_2 R(\xi) - \chi_3 R(\xi)^2)}. \tag{64}$$

Thus, we arrive at the soliton wave profile

$$R(\xi) = \frac{4\chi_1}{\left(4\chi_1\chi_3 + \chi_2^2\right) e^{\sqrt{\chi_1}\kappa\xi} + 2\chi_2 + e^{-\sqrt{\chi_1}\kappa\xi}}, \tag{65}$$

or the bright-dark soliton solution:

$$R(\xi) = \frac{\chi_1\chi_2 \left(\operatorname{sech}\left(\frac{\kappa\xi\sqrt{\chi_1}}{2}\right)\right)^2}{\chi_2^2 - \chi_1\chi_3 \left(1 - \tanh\left(\frac{\kappa\xi\sqrt{\chi_1}}{2}\right)\right)^2}. \tag{66}$$

The combination of (63) with (64) into (9) leaves us with the equations:

$$A_0^3 b - A_0 w = 0, \tag{67}$$

$$2\left(\frac{\chi_1^2\gamma_2 k^4\kappa^4}{2} + \chi_1 k^2\left(aA_0 - \frac{\gamma_3 w}{2}\right)\kappa^2 + \frac{3bA_0^2}{2} - \frac{w}{2}\right)A_1 = 0, \tag{68}$$

$$16\left(\chi_1 A_2 - \frac{15\chi_2 A_1}{32}\right)\chi_1 k^4\gamma_2\kappa^4 + 8k^2\left(\frac{a\chi_1 A_1^2}{2} - \frac{3\left(aA_0 - \frac{\gamma_3 w}{2}\right)\chi_2 A_1}{8} + \chi_1 A_2\left(aA_0 - \frac{\gamma_3 w}{2}\right)\right)\kappa^2$$

$$+ 3bA_0 A_1^2 + 3A_2\left(bA_0^2 - \frac{w}{3}\right) = 0, \tag{69}$$

$$-65\left(\frac{\left(4\chi_1\chi_3 - \frac{3\chi_2^2}{2}\right)A_1}{13} + \chi_1\chi_2 A_2\right)k^4\gamma_2\kappa^4$$

$$+18\left(-\frac{5a\chi_2 A_1^2}{18} + \left(a\chi_1 A_2 - \frac{2\left(aA_0 - \frac{\gamma_3 w}{2}\right)\chi_3}{9}\right)A_1 - \frac{5A_2\left(aA_0 - \frac{\gamma_3 w}{2}\right)\chi_2}{9}\right)k^2\kappa^2 + 6bA_0 A_1 A_2 + bA_1^3 = 0, \tag{70}$$

$$-120\left(-\frac{\chi_2\chi_3 A_1}{4} + A_2\left(\chi_1\chi_3 - \frac{7\chi_2^2}{16}\right)\right)k^4\gamma_2\kappa^4$$

$$+16\left(-\frac{3a\chi_3 A_1^2}{8} - \frac{21a\chi_2 A_1 A_2}{16} + A_2\left(a\chi_1 A_2 - \frac{3\left(aA_0 - \frac{\gamma_3 w}{2}\right)\chi_3}{4}\right)\right)k^2\kappa^2 + 3bA_2\left(A_0 A_2 + A_1^2\right) = 0, \tag{71}$$

$$168\chi_3\left(\chi_2 A_2 + \frac{\chi_3 A_1}{7}\right)k^4\gamma_2\kappa^4 - 18A_2 a\left(\chi_2 A_2 + \frac{4\chi_3 A_1}{3}\right)k^2\kappa^2 + 3bA_1 A_2^2 = 0, \tag{72}$$

$$120A_2\chi_3^2 k^4\kappa^4\gamma_2 - 20A_2^2 a\chi_3 k^2\kappa^2 + A_2^3 b = 0. \tag{73}$$

Upon solving these equations, one uncovers the outcomes:

$$A_0 = 0, \quad A_1 = -\frac{10\chi_2 ak^2\kappa^2\chi_3}{b\left(\chi_2^2 k^2\kappa^2\gamma_3 - 5\chi_3\right)}, \quad A_2 = -\frac{20ak^2\kappa^2\chi_3^2}{b\left(\chi_2^2 k^2\kappa^2\gamma_3 - 5\chi_3\right)},$$

$$\chi_1 = -\frac{\chi_2^2}{4\chi_3}, \quad w = \frac{5k^4\kappa^4 a^2\chi_2^4}{6b\left(\chi_2^2 k^2\kappa^2\gamma_3 - 5\chi_3\right)^2}, \quad \gamma_2 = -\frac{10a^2\chi_3\left(\chi_2^2 k^2\kappa^2\gamma_3 - 4\chi_3\right)}{3b\left(\chi_2^2 k^2\kappa^2\gamma_3 - 5\chi_3\right)^2}. \tag{74}$$

The inclusion of (74) with the help of (66) into (63) results in the bright-dark soliton wave profile:

$$q(x,t)$$

$$= -\frac{10\chi_2^2 k^2 a\kappa^2 \operatorname{sech}^2\left(\frac{\kappa kx\sqrt{-\frac{\chi_2^2}{\chi_3}}}{4}\right)\left(2\operatorname{sech}^2\left(\frac{\kappa kx\sqrt{-\frac{\chi_2^2}{\chi_3}}}{4}\right)+\tanh^2\left(\frac{\kappa kx\sqrt{-\frac{\chi_2^2}{\chi_3}}}{4}\right)-2\tanh\left(\frac{\kappa kx\sqrt{-\frac{\chi_2^2}{\chi_3}}}{4}\right)-3\right)}{b\left(\chi_2^2 k^2\kappa^2\gamma_3-5\chi_3\right)\left(\tanh^2\left(\frac{\kappa kx\sqrt{-\frac{\chi_2^2}{\chi_3}}}{4}\right)-2\tanh\left(\frac{\kappa kx\sqrt{-\frac{\chi_2^2}{\chi_3}}}{4}\right)-3\right)^2}$$

$$\times e^{\frac{i}{6}\frac{\left(6\theta b\left(\chi_2^2 k^2\kappa^2\gamma_3-5\chi_3\right)^2+5k^4\kappa^4 a^2\chi_2^4 t\right)}{b\left(\chi_2^2 k^2\kappa^2\gamma_3-5\chi_3\right)^2}}. \tag{75}$$

The wave profile, as characterized in (75), is defined as

$$\chi_3 < 0. \tag{76}$$

3. Results and discussion

This section presents a comprehensive analysis of quiescent soliton solutions derived from the RKL equation. Figures 1 through 4 depict different soliton structures, dark, singular, bright, and bright-dark solitons, under varying inverse width parameters k. The fixed parameters $A_2 = 1$, $K = e$, $\chi = 1$, $a = 1$, $\kappa = 1$, and $\chi_2 = 1$ are applied consistently across all figures, ensuring a controlled environment for studying the effect of k. Each figure explores the influence of increasing k values: $k = 1$, 1.5, 1.9, 2.4, 2.9, 3.8, 4.8, 7.

Figure 1 illustrates the modulus of the quiescent dark soliton described by equation (40). Dark solitons are characterized by a localized dip in intensity against a uniform background, a signature trait resulting from destructive interference. The 2D plots depict how the soliton evolves as the inverse width parameter k increases. At $k = 1$, the soliton manifests as a broad, shallow dip. As k increases to $k = 1.5$ and $k = 1.9$, the soliton narrows, and the minimum intensity deepens, reflecting stronger localization. By $k = 2.9$, the soliton dip becomes more distinct, with sharper gradients along the soliton edges. At $k = 4.8$ and $k = 7$, the soliton width is significantly reduced, and the dip nears zero at the center, representing maximum intensity depletion. This progressive narrowing aligns with the well-established property of dark solitons, where k directly correlates with inverse soliton width. Physically, increasing k corresponds to stronger nonlinearity or reduced dispersion. The sharper dips at higher k values indicate a more pronounced phase shift across the soliton, critical for applications in optical communication, where dark solitons are employed to maintain signal stability over long distances.

Figure 2 visualizes the modulus of the quiescent singular soliton governed by equation (41). Singular solitons, unlike their regular counterparts, exhibit an amplitude peak that diverges at the soliton center, reflecting infinite localization. At $k = 1$, the soliton exhibits a sharp central peak with finite side lobes. As k increases, the soliton becomes steeper and more confined around the center, with the side lobes diminishing in intensity. At $k = 3.8$ and beyond, the peak approaches

singularity, sharply rising while the surrounding field approaches near-zero levels. By $k = 7$, the singular soliton is highly localized, demonstrating intense energy concentration at the central point. The singularity represents a scenario where nonlinear effects dominate over dispersion, producing self-focusing phenomena. This solution is crucial for modeling phenomena like filamentation in nonlinear optics and self-focusing in plasma physics. The robustness of the singular soliton across varying k values reinforces the stability of the derived analytical solution, indicating its feasibility for practical physical systems.

Figure 3 highlights the modulus of the quiescent bright soliton, dictated by equation (62). Bright solitons represent localized peaks of light intensity within a low background, a fundamental feature arising from constructive interference. At $k = 1$, the bright soliton appears as a wide, shallow peak. Increasing k to 1.5 and 1.9 results in a noticeable sharpening of the peak. By $k = 2.9$, the soliton profile becomes narrow, with enhanced amplitude at the center. At $k = 7$, the soliton is tightly confined, demonstrating maximum localization with minimal side lobes. The growth in amplitude with increasing k underscores the role of inverse width in intensifying soliton strength. The bright soliton's evolution under varying k showcases its adaptability in highly dispersive or nonlinear media. Bright solitons are integral to nonlinear fiber optics, where they enable the transmission of intense, localized light pulses without spreading. The observed narrowing and peak growth at higher k values align with physical expectations for bright solitons in environments with increasing nonlinearity or decreasing dispersion.

Figure 4 depicts the modulus of the quiescent bright-dark soliton described by equation (75). This soliton structure merges features of bright and dark solitons, resulting in a hybrid state where a bright peak exists within a dark soliton dip. At $k = 1$, the bright component is broad and shallow, while the surrounding dark dip is gentle. As k increases, the bright peak narrows and intensifies, while the dark soliton's depth increases. By $k = 3.8$, the bright peak is sharply confined, and the dark dip becomes prominent, creating a high-contrast bright-dark profile. At $k = 7$, the bright soliton component is maximally localized, and the dark background reaches near-zero intensity at the center. Bright-dark solitons are essential in applications involving multicomponent fields, where intensity modulation between bright and dark regions can facilitate optical switching and data encoding. The ability to control the balance between the bright and dark components by tuning k suggests potential use in photonic circuits and optical lattices. The coexistence of bright and dark states enhances the soliton's stability, enabling applications in optical fiber systems that require complex modulation formats.

Across Figures 1-4, the inverse width parameter k consistently governs soliton localization, amplitude, and profile sharpness. The trend of narrowing solitons with increasing k is evident in all soliton types, emphasizing the central role of this parameter in controlling soliton dynamics. This universal behavior highlights the adaptability of the RKL equation in modeling diverse soliton structures, demonstrating its relevance for practical applications in nonlinear optics, waveguide design, and optical communication systems. The results confirm that quiescent soliton solutions derived from the RKL equation provide a rich mathematical framework for studying soliton interactions under various nonlinear and dispersive conditions, reinforcing the equation's significance in contemporary photonic research.

4. Conclusions

This study has presented a comprehensive analysis of solitary wave solutions to the perturbed RKL equation, which serves as a versatile model for nonlinear wave propagation in various physical systems. By employing three advanced analytical techniques, which are the METFM, the addendum to Kudryashov method, and the Kudryashov's auxiliary equation method, we successfully derived a broad spectrum of solitary wave solutions. These include dark solitons, bright solitons, singular solitons, and hybrid bright-dark solitons, each characterized by unique structural and dynamical properties.

The novelty of this work lies in the identification of quiescent solitary wave solutions, which have not been previously reported in the context of the RKL equation. These solutions expand the equation's known solution space and reveal new dynamical regimes governed by the interplay of various physical effects. The RKL equation incorporates nonlinear CD, higher-order dispersion terms (such as third- and fourth-order dispersion), self-steepening, self-frequency shift, and

spatio-temporal terms. This richness makes it an exceptional framework for modeling the behavior of nonlinear waves in environments such as optical fibers, plasmas, and fluid systems.

The solutions derived here provide deeper insights into the underlying mechanisms that govern nonlinear wave dynamics. For example: Bright solitons illustrate the balance between nonlinearity and anomalous dispersion, creating localized peaks that maintain their energy over long distances. Dark solitons arise from the interaction of normal dispersion with nonlinearity, forming intensity dips on a continuous wave background. Singular solitons showcase unique mathematical features, with solutions that exhibit singularities under specific conditions. Hybrid bright-dark solitons highlight the coexistence of opposing characteristics, further enriching the diversity of waveforms possible in nonlinear systems.

To emphasize the physical relevance of these solutions, detailed two-dimensional graphical representations were presented. These plots visualize the structural features of each soliton type, providing intuitive insights into their spatial behaviors. Such visualizations not only aid in understanding the solutions themselves but also highlight their potential implications for real-world applications. For instance, bright solitons are critical for optical communication systems due to their stability, while dark solitons are significant in hydrodynamic and plasma studies.

From a practical perspective, the findings of this study hold promise for a range of applications. The stability and energy-preserving characteristics of the solitary wave solutions make them ideal candidates for high-capacity data transmission in nonlinear optical fibers. The unique properties of the derived solitons could be utilized in advanced signal processing techniques, including soliton-based filters and modulators. Singular and hybrid solitons could serve as models for localized energy transport in plasma, fluid dynamics, and other nonlinear systems. From a theoretical standpoint, this study enhances the understanding of the RKL equation as a unifying model for nonlinear wave dynamics. The methods used here demonstrate the efficacy of advanced analytical techniques in uncovering novel solutions to complex equations, thereby expanding the analytical toolkit available for researchers.

While this study has successfully derived and characterized an extensive set of solitary wave solutions, several avenues for future research remain open: Future studies could explore additional physical effects, such as inhomogeneities, external potentials, or multi-dimensional extensions of the RKL equation, to uncover even richer solution spaces. Also, experimental efforts in optical fibers, plasmas, or fluid systems could validate the practical relevance of these solutions, bridging the gap between theory and real-world applications [26–30].

In conclusion, this work makes significant contributions to the study of nonlinear wave dynamics by expanding the known solution space of the perturbed RKL equation. The solitary wave solutions derived here not only deepen the theoretical understanding of nonlinear systems but also highlight the practical potential of these solutions in advanced technologies. By addressing both analytical techniques and physical implications, this study underscores the RKL equation's versatility as a model for investigating and leveraging the complex interplay of nonlinearity and dispersion in diverse applications. This research sets the stage for future explorations of the RKL equation and similar nonlinear systems, paving the way for both theoretical advancements and practical innovations.

Acknowledgement

One of the authors, AB, is grateful to Grambling State University for the financial support he received as the Endowed Chair of Mathematics. This support is sincerely appreciated.

Conflict of interest

The authors claim that there is no conflict of interest.

References

[1] Ren B, Lin J. The integrability of a (2 + 1)-dimensional nonlinear wave equation: Painlevé property, multi-order breathers, multi-order lumps and hybrid solutions. *Wave Motion*. 2023; 117: 103110. Available from: https://doi.org/10.1016/j.wavemoti.2022.103110.

[2] Hussain A, Usman M, Al-Sinan BR, Osman WM, Ibrahim TF. Symmetry analysis and closed-form invariant solutions of the nonlinear wave equations in elasticity using optimal system of Lie subalgebra. *Chinese Journal of Physics*. 2023; 83: 1-13. Available from: https://doi.org/10.1016/j.cjph.2023.02.011.

[3] Adem AR, Podile TJ, Muatjetjeja B. A generalized (3 + 1)-dimensional nonlinear wave equation in liquid with gas bubbles: symmetry reductions; exact solutions; conservation laws. *International Journal of Applied and Computational Mathematics*. 2023; 9(5): 82. Available from: https://doi.org/10.1007/s40819-023-01533-3.

[4] Adeyemo OD, Khalique CM. Lie group theory, stability analysis with dispersion property, new soliton solutions and conserved quantities of 3D generalized nonlinear wave equation in liquid containing gas bubbles with applications in mechanics of fluids, biomedical sciences and cell biology. *Communications in Nonlinear Science and Numerical Simulation*. 2023; 123: 107261. Available from: https://doi.org/10.1016/j.cnsns.2023.107261.

[5] Kumar S, Hamid I, Abdou MA. Specific wave profiles and closed-form soliton solutions for generalized nonlinear wave equation in (3 + 1)-dimensions with gas bubbles in hydrodynamics and fluids. *Journal of Ocean Engineering and Science*. 2023; 8(1): 91-102. Available from: https://doi.org/10.1016/j.joes.2021.12.003.

[6] Arnous AH, Mirzazadeh M, Akinyemi L, Akbulut A. New solitary waves and exact solutions for the fifth-order nonlinear wave equation using two integration techniques. *Journal of Ocean Engineering and Science*. 2023; 8(5): 475-480. Available from: https://doi.org/10.1016/j.joes.2022.02.012.

[7] Vivas-Cortez M, Raza N, Kazmi SS, Chahlaoui Y, Basendwah GA. A novel investigation of dynamical behavior to describe nonlinear wave motion in (3 + 1)-dimensions. *Results in Physics*. 2023; 55: 107131. Available from: https://doi.org/10.1016/j.rinp.2023.107131.

[8] Zhao Z, He L, Wazwaz AM. Dynamics of lump chains for the BKP equation describing propagation of nonlinear waves. *Chinese Physics B*. 2023; 32(4): 040501. Available from: https://doi.org/10.1088/1674-1056/acb0c1.

[9] Wallauch D. Strichartz estimates and blowup stability for energy critical nonlinear wave equations. *Transactions of the American Mathematical Society*. 2023; 376(6): 4321-4360. Available from: https://doi.org/10.1090/tran/8879.

[10] Cerrai S, Xie M. On the small noise limit in the Smoluchowski-Kramers approximation of nonlinear wave equations with variable friction. *Transactions of the American Mathematical Society*. 2023; 376(11): 7651-7689. Available from: https://doi.org/10.1090/tran/8946.

[11] Biswas A. 1-soliton solution of the generalized Radhakrishnan, Kundu, Lakshmanan equation. *Physics Letters A*. 2009; 373(30): 2546-2548. Available from: https://doi.org/10.1016/j.physleta.2009.05.010.

[12] Kudryashov NA. Solitary waves of the generalized Radhakrishnan-Kundu-Lakshmanan equation with four powers of nonlinearity. *Physics Letters A*. 2022; 448: 128327. Available from: https://doi.org/10.1016/j.physleta.2022.128327.

[13] Ghanbari B, Gómez-Aguilar JF. Optical soliton solutions for the nonlinear Radhakrishnan-Kundu-Lakshmanan equation. *Modern Physics Letters B*. 2019; 33(32): 1950402. Available from: https://doi.org/10.1142/S0217984919504025.

[14] Tarla S, Ali KK, Yilmazer R, Osman MS. The dynamic behaviors of the Radhakrishnan-Kundu-Lakshmanan equation by Jacobi elliptic function expansion technique. *Optical and Quantum Electronics*. 2022; 54(5): 292. Available from: https://doi.org/10.1007/s11082-022-03710-y.

[15] Wang KJ, Si J. Optical solitons to the Radhakrishnan-Kundu-Lakshmanan equation by two effective approaches. *The European Physical Journal Plus*. 2022; 137(9): 1016. Available from: https://doi.org/10.1140/epjp/s13360-022-03239-9.

[16] Hussain Z, Rehman ZU, Abbas T, Smida K, Le QH, Abdelmalek Z, et al. Analysis of bifurcation and chaos in the traveling wave solution in optical fibers using the Radhakrishnan-Kundu-Lakshmanan equation. *Results in Physics*. 2023; 55: 107145. Available from: https://doi.org/10.1016/j.rinp.2023.107145.

[17] Ullah N, Asjad MI, Ur Rehman H, Akgül A. Construction of optical solitons of Radhakrishnan-Kundu-Lakshmanan equation in birefringent fibers. *Nonlinear Engineering*. 2022; 11(1): 80-91. Available from: https://doi.org/10.1515/nleng-2022-0010.

[18] Özkan YS, Yaşar E, Seadawy AR. On the multi-waves, interaction and Peregrine-like rational solutions of perturbed Radhakrishnan-Kundu-Lakshmanan equation. *Physica Scripta*. 2020; 95(8): 085205. Available from: https://doi.org/10.1088/1402-4896/ab9af4.

[19] Wang KJ, Wang GD, Shi F. Diverse optical solitons to the Radhakrishnan-Kundu-Lakshmanan equation for the light pulses. *Journal of Nonlinear Optical Physics & Materials*. 2024; 33(6): 2350074. Available from: https://doi.org/10.1142/S0218863523500741.

[20] Chen C, Li L, Liu W. Some new optical solitons of the generalized Radhakrishnan-Kundu-Lakshmanan equations with powers of nonlinearity. *Symmetry*. 2022; 14(12): 2626. Available from: https://doi.org/10.3390/sym14122626.

[21] Yıldırım Y, Biswas A, Asiri A. Quiescent optical solitons for the perturbed Radhakrishnan-Kundu-Lakshmanan equation with nonlinear chromatic dispersion. *Journal of Applied Science and Engineering*. 2023; 27(6): 2605-2617. Available from: https://doi.org/10.6180/jase.202406_27(6).0002.

[22] Ozisik M, Cinar M, Secer A, Bayram M. Optical solitons with Kudryashov's sextic power-law nonlinearity. *Optik*. 2022; 261: 169202. Available from: https://doi.org/10.1016/j.ijleo.2022.169202.

[23] Alotaibi H. Traveling wave solutions to the nonlinear evolution equation using expansion method and addendum to Kudryashov's method. *Symmetry*. 2021; 13(11): 2126. Available from: https://doi.org/10.3390/sym13112126.

[24] Cakicioglu H, Ozisik M, Secer A, Bayram M. Optical soliton solutions of Schrödinger-Hirota equation with parabolic law nonlinearity via generalized Kudryashov algorithm. *Optical and Quantum Electronics*. 2023; 55(5): 407. Available from: https://doi.org/10.1007/s11082-023-04634-x.

[25] Onder I, Secer A, Bayram M. Optical soliton solutions of time-fractional coupled nonlinear Schrödinger system via Kudryashov-based methods. *Optik*. 2023; 272: 170362. Available from: https://doi.org/10.1016/j.ijleo.2022.170362.

[26] Li N, Xu S, Sun Y, Chen Q. Bright and dark solitons under spatiotemporal modulation in (2 + 1)-dimensional Spin-1 Bose-Einstein condensates. *Nonlinear Dynamics*. 2025; 113(1): 767-782. Available from: https://doi.org/10.1007/s11071-024-10243-4.

[27] Yang A, Xu S, Liu H, Li N, Sun Y. Predicting the soliton dynamics and system parameters in optical fiber couplers. *Nonlinear Dynamics*. 2025; 113(2): 1523-1537. Available from: https://doi.org/10.1007/s11071-024-10235-4.

[28] Jiang L. A fast and accurate circle detection algorithm based on random sampling. *Future Generation Computer Systems*. 2021; 123: 245-256. Available from: https://doi.org/10.1016/j.future.2021.05.010.

[29] Zhang H, Manafian J, Singh G, Ilhan OA, Zekiy AO. N-lump and interaction solutions of localized waves to the (2 + 1)-dimensional generalized KP equation. *Results in Physics*. 2021; 25: 104168. Available from: https://doi.org/10.1016/j.rinp.2021.104168.

[30] Chen H, Shahi A, Singh G, Manafian J, Eslami B, Alkader NA. Behavior of analytical schemes with non-paraxial pulse propagation to the cubic-quintic nonlinear Helmholtz equation. *Mathematics and Computers in Simulation*. 2024; 220: 341-356. Available from: https://doi.org/10.1016/j.matcom.2024.02.003.